Available online at www.elixirpublishers.com (Elixir International Journal)

Applied Mathematics

Elixir Appl. Math. 43 (2012) 6520-6527

ISSN: 2229-712X

Effects of chemical reactions on free convection MHD flow past an exponentially accelerated infinite vertical plate through a porous medium with variable temperature and mass diffusion

U S Rajput and P K Sahu

Department of Mathematics and Astronomy, University of Lucknow, Lucknow,U.P.-226007, India.

ARTICLE INFO

Article history:
Received: 4 November 2011;
Received in revised form:
19 January 2012;
Accepted: 31 January 2012;

Keywords
Heat and Mass Transfer,
MHD, Chemical Reaction,
Porous Medium,
Exponentially Accelerated Vertical plate.

ABSTRACT

The effects of chemical reactions on free convection MHD flow of an incompressible, viscous, electrically conducting fluid past an exponentially accelerated infinite vertical plate through a porous medium with variable temperature and mass diffusion is discussed. The plate temperature and the concentration level near the plate increase linearly with time. The magnetic lines of force are assumed to be fixed relative to the plate. The Laplace transform method has been used to find the solutions for the velocity, temperature and concentration profiles. The effects of the various parameters such as Prandtl number, Schmidt number, time, magnetic parameter, permeability parameter, thermal Grashof number, mass Grashof number, accelerating parameter and chemical reaction parameter for velocity, temperature, and concentration and skin-friction profiles have been discussed in detail with the help of graphical representation. The numerical values of skin-friction, Nusselt number and Sherwood number have been tabulated.

Introduction

The application of Hydromagnetic incompressible viscous flow in science and engineering involving heat and mass transfer under the influence of chemical reaction is of great importance to many areas of science and engineering. This frequently occurs in petro-chemical industry, power and cooling system, chemical vapour deposition on surfaces, cooling of nuclear reactors, heat exchanger design, forest fire dynamics and geophysics as well as in magnetohydrodynamic power generation systems. The influence of magnetic field on viscous, incompressible and electrically conducting fluid is of great importance in many applications such as magnetic material processing, glass manufacturing control processes and purification of crude oil etc. Gupta et al. [1] studied free convection on flow past a linearly accelerated vertical plate in the presence of viscous dissipative heat using perturbation method. Kafousias and raptis [7] extended this problem to include mass transfer effects subjected to variable suction or injection. Singh and Kumar [2] have presented free convection effects on flow past an exponentially accelerated vertical plate. Soundalgekar et al. [15] have studied mass transfer effects on the flow past an impulsively started infinite vertical plate with variable temperature or constant heat flux. Hossain and Shayo [6] have presented the skin-friction for accelerated vertical plate. BK Jha [3] has studied MHD free convection and mass transform flow through a porous medium. Jha et al. [4] have studied mass transfer effects on the flow past an exponentially accelerated infinite vertical plate with constant heat flux and uniform mass diffusion. Reddy et al. [9] have studied the unsteady mixed convective mass transfer flow of a viscous incompressible and electrically conducting fluid past an accelerated infinite vertical porous flat plate with suction in the presence of transverse magnetic field. Muthucumaraswamy et al. [8] have studied mass transfer effects on exponentially accelerated isothermal vertical plate. Rajesh [14] has presented the effect of a uniform transverse magnetic field on the free convection and mass transform flow of an electrically conducting fluid past an exponentially accelerated infinite vertical plate through a porous medium with variable temperature. Earlier, we have already studied four MHD models, namely (i) unsteady transient free convection MHD flow of an incompressible viscous electrically conducting fluid between two infinite vertical parallel plates with constant temperature and variable mass diffusion [10], (ii) unsteady transient free convection MHD flow of an incompressible viscous electrically conducting fluid between two infinite vertical parallel plates with variable temperature and uniform mass diffusion in a porous medium [11], (iii) the influence of first order homogeneous chemical reactions on unsteady transient free convection flow of a viscous, incompressible, electrically conducting fluid between two long vertical parallel plates through a porous medium with heat generation/absorption in the presence of transverse magnetic field [12] and (iv) the combined effects of radiation and heat generation/absorption on steady hydromagnetic flow of an electrically conducting optically thin fluid through a vertical channel filled with porous medium and non-uniform wall temperatures [13]. Kumar and Verma [5] investigated the effects of radiation on unsteady MHD flow of an electrically conducting radiating, viscous, incompressible fluid past an impulsively started moving exponentially accelerated vertical plate with variable temperature in the presence of heat generation and applied transverse magnetic field.

The objective of the present paper is to investigate the effect of chemical reaction and uniform transverse magnetic field (fixed relative to the plate) on the free convection flow past an exponentially accelerated vertical plate through a porous medium with variable temperature and mass diffusion

Tele:
E-mail addresses: rajputpradeeplko@gmail.com

Mathematical Analysis:

In this paper, we have considered the unsteady free convection MHD flow of an incompressible, viscous, electrically conducting fluid past an exponentially accelerated infinite vertical plate through a porous medium with variable temperature and mass diffusion in the presence of chemical reaction. We assume that the magnetic Reynolds number of fluid is taken so small that the effect of induced magnetic field is negligible in comparison to the applied one. A magnetic field of uniform strength B_0 is applied normal to the plate. The flow is assumed to be in x'-direction which is taken along the vertical plate in upward direction. The y'-axis is taken to be normal to the plate. Initially, the temperature of the fluid and plate are same T'_∞ in the stationary condition and the concentration of the fluid is C'_∞. At time $t'>0$, the plate is exponentially accelerated with a velocity $u_0\exp(a't')$ in its own plane and at the same time the plate temperature and the concentration level near the plate increase linearly with time t. The governing equations under the usual Boussinesq's approximation are as follows:

$$\frac{\partial u'}{\partial t'}=g\beta(T'-T'_\infty)+g\beta^*(C'-C'_\infty)+\nu\frac{\partial^2 u'}{\partial y'^2}-\frac{\sigma B_0^2}{\rho}(u'-u_0e^{a't'})-\frac{\nu}{K'}u', \tag{1}$$

$$\rho C_p\frac{\partial T'}{\partial t'}=k\frac{\partial^2 T'}{\partial y'^2}, \tag{2}$$

$$\frac{\partial C'}{\partial t'}=D\frac{\partial^2 C'}{\partial y'^2}-K^*(C'-C'_\infty). \tag{3}$$

The initial and boundary conditions are as follows:

$$\left.\begin{aligned}
&t'\le 0:\ u'=0,\quad T'=T'_\infty,\quad C'=C'_\infty\quad \text{for all } y',\\
&t'>0:\ u'=u_0e^{a't'},\ T'=T'_\infty+(T'_w-T'_\infty)At',\\
&\qquad C'=C'_\infty+(C'_w-C'_\infty)At'\quad \text{at}\quad y'=0,\\
&\qquad u'=0,\ T'\to T'_\infty,\ C'\to C'_\infty\quad \text{as}\quad y'\to\infty,
\end{aligned}\right\} \tag{4}$$

where $A=\dfrac{u_0^2}{\nu}$.

Introducing the following non-dimensional quantities:

$$\left.\begin{aligned}
&y=\frac{y'u_0}{\nu},\ t=\frac{t'u_0^2}{\nu},\ u=\frac{u'}{u_0},\ Gr=\frac{g\beta\nu(T'_w-T'_\infty)}{u_0^3},\ \theta=\frac{T'-T'_\infty}{T'_w-T'_\infty},\\
&\Pr=\frac{\mu C_p}{k}, C=\frac{C'-C'_\infty}{C'_w-C'_\infty},\ Gm=\frac{g\beta^*\nu(C'_w-C'_\infty)}{u_0^3},\ Sc=\frac{\nu}{D},\\
&M=\frac{\sigma B_0^2\nu}{\rho u_0^2},\ \mu=\rho\nu,\ a=\frac{a'\nu}{u_0^2}, K=\frac{u_0^2K'}{\nu^2}, F=\frac{K^*\nu}{u_0^2},
\end{aligned}\right\} \tag{5}$$

Then the model is transformed in to the following non-dimensional form of equations:

$$\frac{\partial u}{\partial t}=Gr\theta+GmC+\frac{\partial^2 u}{\partial y^2}-M(u-e^{at})-\frac{u}{K}, \tag{6}$$

$$\frac{\partial\theta}{\partial t}=\frac{1}{\Pr}\frac{\partial^2\theta}{\partial y^2}, \tag{7}$$

$$\frac{\partial C}{\partial t}=\frac{1}{Sc}\frac{\partial^2 C}{\partial y^2}-FC. \tag{8}$$

The initial and boundary conditions become:

$$\left.\begin{aligned}
&t\le 0:\ u=0,\quad \theta=0,\quad C=0\quad \text{for all}\quad y,\\
&t>0:\ u=e^{at},\ \theta=t,\quad C=t\quad \text{at}\quad y=0,\\
&\qquad u=0,\quad \theta\to 0,\quad C\to 0\quad \text{at}\quad y\to\infty.
\end{aligned}\right\} \tag{9}$$

Applying the Laplace transform in equations (6), (7) and (8), we have:

$$\frac{d^2\bar u}{dy^2}-(H+s)\bar u=-Gr\bar\theta-Gm\bar C-\frac{M}{s-a}, \tag{10}$$

$$\frac{d^2\bar\theta}{dy^2}-s\Pr\bar\theta=0, \tag{11}$$

$$\frac{d^2\bar C}{dy^2}-(F+s)Sc\bar C=0. \tag{12}$$

The boundary condition becomes:

$$\left.\begin{aligned}
&t>0:\ \bar u=\frac{1}{s-a},\ \bar\theta=\frac{1}{s^2},\ \bar C=\frac{1}{s^2}\quad \text{at}\ y=0,\\
&\qquad \bar u=0,\quad \bar\theta=0,\quad \bar C=0\quad \text{as}\ y\to\infty.
\end{aligned}\right\} \tag{13}$$

The solution of equations (10), (11) and (12) with the boundary condition (13) are given by

$$\bar u(y,s)=\left[\frac{1}{a_{11}}-\frac{M}{a_{12}}+\frac{Gr}{a_{13}}+\frac{Gm}{a_{14}}\right]e^{-y\sqrt{s+H}}$$

$$-\frac{Gre^{-y\sqrt{s\Pr}}}{a_{13}}-\frac{Gme^{-y\sqrt{(F+s)Sc}}}{a_{14}}+\frac{M}{a_{12}}, \tag{14}$$

$$\bar\theta(y,s)=\frac{e^{-y\sqrt{s\Pr}}}{s^2}, \tag{15}$$

$$\bar C(y,s)=\frac{e^{-y\sqrt{(F+s)Sc}}}{s^2}, \tag{16}$$

where $\bar u(y,s)=\int_0^\infty e^{-st}u(y,t)dt;\ (s>0),\ s$ being Laplace transform parameter,

$a_{11}=(s-a), a_{12}=(s-a)(s+H),$

$a_{13}=s^2\left[s(\Pr-1)-H\right]$ and $a_{14}=s^2\left[s(Sc-1)-L\right].$

Taking the inverse Laplace transform of equations (14), (15) and (16), the velocity, temperature and concentration fields are given by the expressions:

$$u(y,t)=\left[1-\frac{M}{c_1}\right]\frac{e^{at}}{2}\left[e^{-y\sqrt{c_1}}erfc(\eta-\sqrt{c_1t})+e^{y\sqrt{c_1}}erfc(\eta+\sqrt{c_1t})\right]$$

$$+\frac{Gre^{Rt}}{2HR}\left[e^{-y\sqrt{c_2}}erfc(\eta-\sqrt{c_2t})+e^{y\sqrt{c_2}}erfc(\eta+\sqrt{c_2t})\right]$$

$$-\left[\frac{Gr}{2HR}+\frac{Gm}{2LQ}\right]\left[e^{-y\sqrt{H}}erfc(\eta-\sqrt{Ht})+e^{y\sqrt{H}}erfc(\eta+\sqrt{Ht})\right]$$

$$-\left[\frac{Gr}{2H}+\frac{Gm}{2L}\right]\left[e^{-y\sqrt{H}}erfc(\eta-\sqrt{Ht})c_5+e^{y\sqrt{H}}erfc(\eta+\sqrt{Ht})c_6\right]$$

$$+\frac{Gme^{Qt}}{2LQ}\left[e^{-y\sqrt{c_3}}erfc(\eta-\sqrt{c_3t})+e^{y\sqrt{c_3}}erfc(\eta+\sqrt{c_3t})\right]$$

$$-\frac{Gre^{Rt}}{2HR}\left[e^{-y\sqrt{\Pr R}}erfc(\phi-\sqrt{Rt})+e^{y\sqrt{\Pr R}}erfc(\phi+\sqrt{Rt})\right]$$

$$+\frac{Gr}{HR}erfc\left(\frac{y\sqrt{\Pr}}{2\sqrt{t}}\right)+\frac{Gr}{H}\left[\left(t+\frac{y^2\Pr}{2}\right)erfc(\phi)-\left(y\sqrt{\frac{t\Pr}{\pi}}\right)e^{-\frac{y^2\Pr}{4t}}\right]$$

$$-\frac{Gme^{Qt}}{2LQ}\left[e^{-y\sqrt{c_4Sc}}erfc(\psi-\sqrt{c_4t})+e^{y\sqrt{c_4Sc}}erfc(\psi+\sqrt{c_4t})\right]$$

$$+\frac{Gm}{2LQ}\left[e^{-y\sqrt{FSc}}erfc(\psi-\sqrt{Ft})+e^{y\sqrt{FSc}}erfc(\psi+\sqrt{Ft})\right]$$

$$+\frac{Gm}{2L}\left[e^{-y\sqrt{FSc}}erfc(\psi-\sqrt{Ft})c_7+e^{y\sqrt{FSc}}erfc(\psi+\sqrt{Ft})c_8\right]$$

$$+\frac{M}{a+H}\left[e^{at}-e^{-Ht}\right]+\frac{Me^{-Ht}}{c_1}erfc\left(\frac{y}{2\sqrt{t}}\right), \tag{17}$$

$$\theta(y,t)=\left[\left(t+\frac{y^2\Pr}{2}\right)erfc(\phi)-\left(y\sqrt{\frac{t\Pr}{\pi}}\right)e^{-\frac{y^2\Pr}{4t}}\right], \qquad (18)$$

$$C(y,t)=\frac{1}{2}\left[e^{-y\sqrt{FSc}}erfc(\psi-\sqrt{Ft})c_7+e^{y\sqrt{FSc}}erfc(\psi+\sqrt{Ft})c_8\right]. \qquad (19)$$

where $H=M+\frac{1}{K}, L=H-FSc, R=\frac{H}{\Pr-1}$ with $\Pr\neq 1$, $Q=\frac{L}{Sc\text{-}1}$ with $\Pr\neq 1$,

$$c_1=a+H, c_2=H+R, c_3=H+Q, c_4=F+Q, c_5=\left(t-\frac{y}{2\sqrt{H}}\right), c_6=\left(t+\frac{y}{2\sqrt{H}}\right),$$

$$c_7=\left(t-\frac{y\sqrt{Sc}}{2\sqrt{F}}\right), c_8=\left(t+\frac{y\sqrt{Sc}}{2\sqrt{F}}\right), \eta=\frac{y}{2\sqrt{t}},\ \phi=\frac{y\sqrt{\Pr}}{2\sqrt{t}} \text{ and } \psi=\frac{y\sqrt{Sc}}{2\sqrt{t}}.$$

Using Eqs (17), (18) and (19), the skin-friction (τ), the rate of heat transfer (Nu) and the rate of mass transfer (Sh) in non-dimensional form are defined as

3- Skin-friction:

$$\tau'=-\mu\left(\frac{\partial u'}{\partial y'}\right)_{y'=0}$$

Which by virtue of (5) reduce to

$$\tau=\frac{\tau'}{\rho u_0^2}=-\left(\frac{\partial u}{\partial y}\right)_{y=0}$$

$$=\frac{e^{-Ht}M}{c_1\sqrt{\pi t}}+\frac{e^{at}}{2}\left[1-\frac{M}{c_1}\right]\left[\frac{2e^{-c_1t}}{\sqrt{\pi t}}+\sqrt{c_1}\left\{erfc\left(-\sqrt{c_1t}\right)-erfc\left(\sqrt{c_1t}\right)\right\}\right]$$

$$+\frac{e^{Qt}Gm}{2LQ}\left[\frac{2e^{-c_3t}}{\sqrt{\pi t}}+\sqrt{c_3}\left\{erfc\left(-\sqrt{c_3t}\right)-erfc\left(\sqrt{c_3t}\right)\right\}\right]$$

$$+\frac{Gm}{2LQ}\left[\frac{2\sqrt{Sct}e^{-Ft}}{\sqrt{\pi}}+\sqrt{ScF}\left\{erfc\left(-\sqrt{Ft}\right)-erfc\left(\sqrt{Ft}\right)\right\}\right]$$

$$+\frac{Gm}{2L}\left[\frac{2\sqrt{Sct}e^{-Ft}}{\sqrt{\pi}}+\frac{\sqrt{Sc}}{2\sqrt{F}}c_9+t\sqrt{ScF}c_9\right]$$

$$-\frac{e^{Qt}Gm}{2LQ}\left[\frac{2\sqrt{Sc}e^{-c_4t}}{\sqrt{\pi t}}+\sqrt{c_4Sc}\left\{erfc\left(-\sqrt{c_4t}\right)-erfc\left(\sqrt{c_4t}\right)\right\}\right]$$

$$+\frac{Gr\sqrt{\Pr}}{HR\sqrt{\pi t}}+\frac{2Gr\sqrt{\Pr t}}{H\sqrt{\pi}}$$

$$-\frac{Gre^{Rt}}{2HR}\left[\frac{2\sqrt{\Pr}e^{-Rt}}{\sqrt{\pi t}}+\sqrt{\Pr R}\left\{erfc\left(-\sqrt{Rt}\right)-erfc\left(\sqrt{Rt}\right)\right\}\right]$$

$$+\frac{Gre^{Rt}}{2HR}\left[\frac{2e^{-c_2t}}{\sqrt{\pi t}}+\sqrt{c_2}\left\{erfc\left(-\sqrt{c_2t}\right)-erfc\left(\sqrt{c_2t}\right)\right\}\right]$$

$$-\left[\frac{Gm}{2L}+\frac{Gr}{2H}\right]\left[\frac{2e^{-Ht}\sqrt{t}}{\sqrt{\pi}}+\frac{1}{2\sqrt{H}}c_{10}+t\sqrt{H}c_{10}\right]$$

$$-\left[\frac{Gm}{2LQ}+\frac{Gr}{2HR}\right]\left[\frac{2e^{-Ht}}{\sqrt{\pi t}}+\sqrt{H}\left\{erfc\left(-\sqrt{Ht}\right)-erfc\left(\sqrt{Ht}\right)\right\}\right], \qquad (20)$$

4- Nusselt Number:

$$Nu=-\left(\frac{\partial\theta}{\partial y}\right)_{y=0}=\frac{2\sqrt{\Pr t}}{\sqrt{\pi}}, \qquad (21)$$

5- Shrewood Number:

$$Sh=-\left(\frac{\partial C}{\partial y}\right)_{y=0}=\frac{1}{2}\left[\frac{2\sqrt{Sct}e^{-Ft}}{\sqrt{\pi}}+\frac{\sqrt{Sc}}{2\sqrt{F}}c_9+t\sqrt{ScF}c_9\right], \qquad (22)$$

where $c_9=\left[erfc\left(-\sqrt{Ft}\right)-erfc\left(\sqrt{Ft}\right)\right], c_{10}=\left[erfc\left(-\sqrt{Ht}\right)-erfc\left(\sqrt{Ht}\right)\right]$.

Result and Discussions:

The numerical values of the velocity u, concentration C, temperature θ, skin-friction τ, Nusselt number Nu and Sherwood number Sh are computed for different parameters like Prandtl number $\Pr$, Schmidt number Sc, magnetic parameter M, thermal Grashof number Gr, mass Grashof number Gm, time t, permeability parameter K, accelerating parameter a and chemical reaction parameter F. The values of main parameters considered are: $\Pr$ = 0.71 (for air), 7 (for water) and 3 (for the saturated liquid Freon at 273.3K); Sc = 0.60 (for Oxygen), 0.78 (for Ammonia) and 2.01 (for Ethyl Benzen); M = 1.0, 2.0, 3.0; Gr = 5, 10, 15 (for cooling of the plate) and -5, -10, -15 (for heating of the plate); K = 0.3, 0.5, 1; a = 0.2, 0.5, 0.9; F = 1, 2, 3, 30 and t = 0.2, 0.4, 0.6. The velocity, temperature, concentration and skin-friction profiles for different parameters $\Pr$, Sc, M, Gr, Gm, t, K, a and F are presented in figures (1) to (18) for heating $(Gr<0)$ and cooling $(Gr>0)$ of the plate. The numerical values for skin-friction, Nusselt number and Shrewood number are shown in tables 1 to 5, 6 and 7, respectively.

Figure-1 shows the effect of time t and Prandtl number $\Pr$ on the temperature of the fluid. It is observed that the temperature for air is greater than that of water and liquid Freon, which is due to the fact that thermal conductivity of fluid decreases with increasing values of the Prandtl number $\Pr$. Also, it is observed that the temperature of the fluid increases with increasing the time.

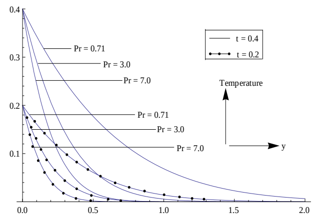

Figure-1: Temperature Profiles

Figure-2 shows the effect of time t and Schmidt number Sc on the concentration of the fluid. The effect of Schmidt number plays an important role in concentration field. It is observed that the concentration of fluid near the surface of the plate increases with decreasing values of the Schmidt number but increases with increasing the time.

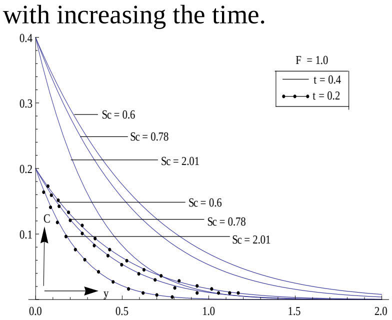

Figure-2: Concentration Profiles

Figure-3 shows the effect of chemical reaction parameter F on the concentration of the fluid. It is observed that the concentration of fluid increases near the surface of the plate with decrease of chemical reaction parameter.

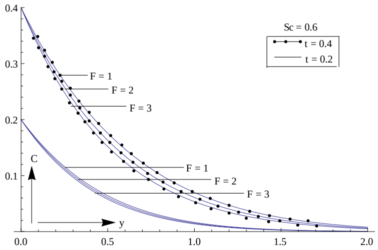

Figure-3: Concentration Profiles

Figures-4, 5, 6 and 7 show the effects of mass Grashof number Gm, accelerating parameter a, permeability parameter K and Prandtl number $\Pr$, respectively, on the velocity of fluid in case of the heating and cooling of the plate at $t = 0.2$. It is observed that the velocity increases with increase of mass Grashof number for the case of cooling of the plate. But the reverse effect is found in case of the heating of the plate. From figures-5 and 6, it is clear that the velocity increases with increase of accelerating and permeability parameters for both the cases cooling and heating of the plate. Figure-7 shows that the velocity increases with decrease of Prandtl number for the case of cooling of the plate. But the reverse effect is found in case of the heating of the plate.

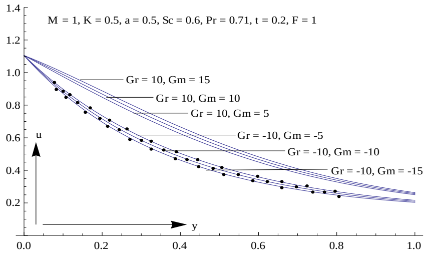

Figure-4: Velocity Profiles

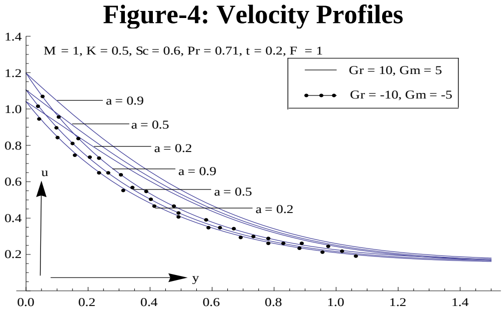

Figure-5: Velocity Profiles

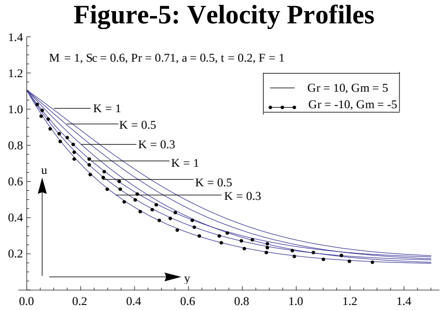

Figure-6: Velocity Profiles

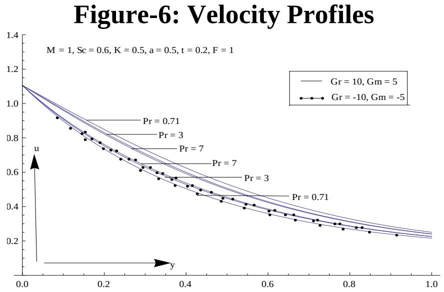

Figure-7: Velocity Profiles

Figures-8, 9 and 10 show the effects of thermal Grashof number Gr, Schmidt number Sc and magnetic parameter M, respectively, on the velocity of fluid in case of the heating and cooling of the plate at $t = 0.2$. It is observed that the velocity increases with increase of thermal grashof number for the case of cooling of the plate. But the reverse effect is found in case of the heating of the plate. From the velocity profile (figure-9) it is observed that the velocity increases with decrease of Schmidt number for the case of cooling of the plate. But the reverse effect is found in case of the heating of the plate. Figure-10 shows that the velocity increases with increase of magnetic parameter for cooling and heating, both.

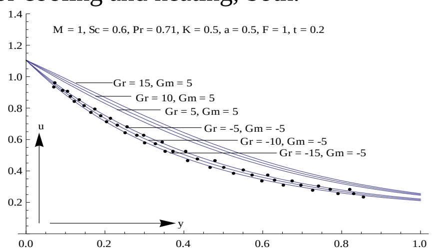

Figure- 8: Velocity Profiles

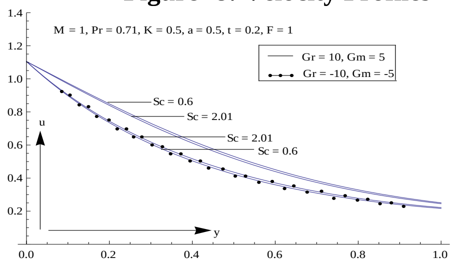

Figure- 9: Velocity Profiles

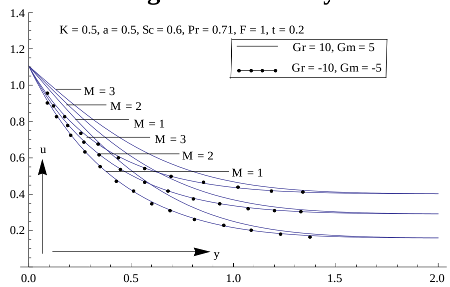

Figure- 10: Velocity Profiles

Figure-11 shows that the velocity increases with increase of time t for the case of cooling of the plate. But the reverse effect is found in case of the heating of the plate. It is also observed that in the case of cooling of the plate, the velocity profile increases near the surface of the plate and becomes maximum and then decreases away from the plate. But reverse trend is observed in case of cooling of the plate.

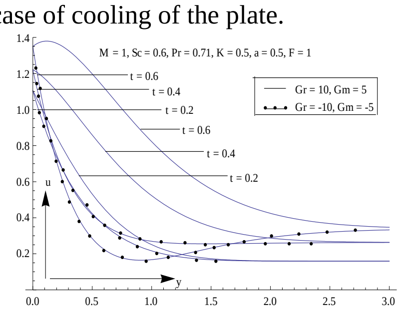

Figure- 11: Velocity Profiles

Figure-12 and Figure-13 show the effect of chemical reaction parameter F on the velocity of fluid for heating and cooling of the plate at $t = 0.2$;

(i) Cooling: The effect is negligible when the difference in the value of F is small but it is visible when the difference is large; for instance, when F = 1, 2, 3 the graphs almost overlap, however profiles shift towards the origin when F = 30.

(ii) Heating: The effect is opposite to that of cooling.

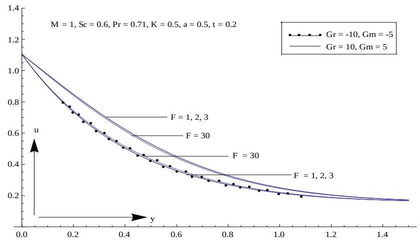

Figure- 12: Velocity Profiles

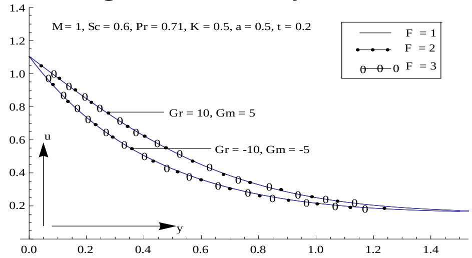

Figure- 13: Velocity Profiles

Figure-14 and Table-1 show the effect of magnetic parameter M on the skin-friction. It is observed that the skin-friction decreases with increase of magnetic parameter in case of both heating and cooling of the plate.

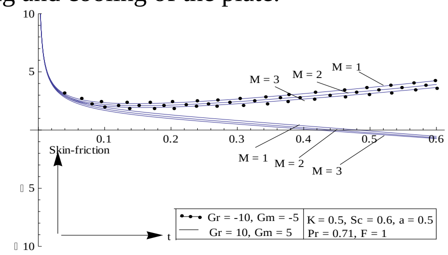

Figure- 14: Skin-friction Profiles

Figure-15 and Table-2 show the effect of chemical reaction parameter F on the skin-friction. These show that the skin-friction decreases with increase of chemical reaction parameter in case of heating of the plate. But the effect is reversed for cooling of the plate.

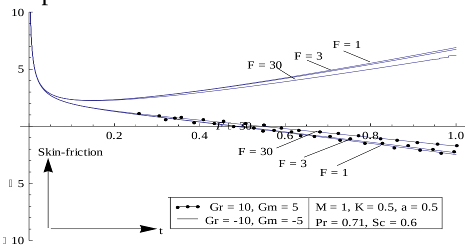

Figure- 15: Skin-friction Profiles

Figure-16 and Table-3 show the effect of Prandtl number $\Pr$ and Schmidt number Sc on the skin-friction. These show that the skin-friction decreases with increase of Prandtl number and Schmidt number in case of heating of the plate. But the reverse effect is found in case of cooling of the plate.

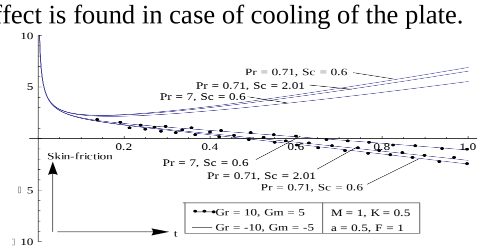

Fig16: Skin-friction Profiles

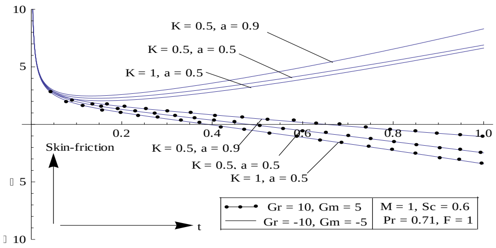

Figure- 17: Skin-friction Profiles

Figure-17 and Table-4 show the effect of permeability parameter K and accelerating parameter a on the skin-friction. These show that the skin-friction increases with increase of accelerating parameter in case of both heating and cooling of the plate. It is also observed that the skin-friction increases with decrease of permeability parameter in case of both heating and cooling of the plate.

Figure-18 and Table-5 show the effect of thermal Grashof number Gr and mass Grashof number Gm on the skin-friction in case of the heating and cooling of the plate. These show that the skin-friction decreases with increase of thermal Grashof number and mass Grashof number in case of cooling of the plate. But the reverse effect is found in case of the heating of the plate.

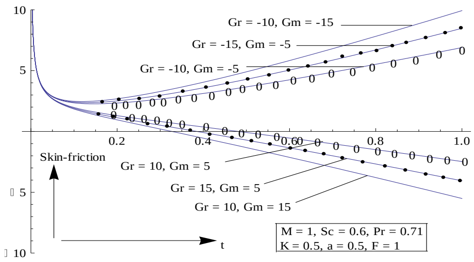

Figure- 18: Skin-friction Profiles

Table-6 shows the effect of Prandtl number $\Pr$ and time t on the Nusselt number Nu. It shows that the Nusselt number increases with increase of Prandtl number and time.

Table-7 shows the effect of chemical reaction parameter F, Schmidt number Sc and time t on the Sherwood number Sh. It shows that the Sherwood number increases with increase of chemical reaction parameter, Schmidt number and time.

Conclusions:

In the present paper, the theoretical solution of free convection MHD flow of an incompressible, viscous, electrically conducting fluid past an exponentially accelerated infinite vertical plate through a porous medium with variable temperature and mass diffusion under the influence of chemical reaction is studied. The solution for the model has been determined by using Laplace transform method. The conclusion of the study is as follows:

- The temperature of fluid increases with decrease of $\Pr$ but increases with increase of time t. The concentration of fluid increase with decrease of Sc and F but increases with increase of time t.
- The velocity increases with increase of Gm, Gr and t for the case of cooling of the plate but the reverse effect is found in case of the heating of the plate.
- The velocity increases with increase of a, K and M for cases, cooling and heating of the plate.
- The velocity increases with decrease of Sc and $\Pr$ for cooling of the plate but the reverse effect is found in case of heating of the plate.

- The effect of F on velocity is negligible when the difference in the value of F is small but it is visible when the difference is large.
- The Nusselt number increases with increase of $\Pr$ time t.
- The Sherwood number increases with increase of F, Sc and time t.
- The skin-friction decreases with increase of M in case of both heating and cooling of the plate. Further, the skin-friction decreases with increase of F, Sc and $\Pr$ in case of heating of plate but the reverse effect is found in case of cooling of the plate.
- Skin-friction increases with increase of a in case of both heating and cooling of the plate. It is also observed that the skin-friction increases with decrease of K in case of both heating and cooling of the plate.
- The skin-friction decreases with increase of Gr and Gm in case of cooling of the plate but the effect is reversed for heating of the plate.

Nomenclature:

u' Velocity component in x'-direction
y' Coordinate axis normal to the plate
t' Time
g Acceleration due to gravity
T' Temperature of the fluid near the plate
T'_∞ Temperature of the fluid for away from the plate
T'_w Temperature of the plate
C' Species concentration in the fluid
C'_∞ Concentration in the fluid for away from the plate
C'_w Concentration in the fluid near the plate
K' Permeability of porous medium
K^* Chemical reaction parameter
u Dimensionless velocity
y Dimensionless Coordinate axis normal to the plate
t Dimensionless time
C_p Specific heat at constant pressure
k Thermal conductivity of the fluid
B_0 External magnetic field
A Constant
a Accelerating parameter
u_0 Velocity of the plate
$\Pr$ Prandtl number
Sc Schmidt number
Gm Mass Grashof number
Gr Thermal Grashof number
D Chemical molecular diffusivity
M Magnetic parameter
F Dimensionless chemical reaction parameter
K Permeability parameter.

Greek Symbols:

β Volumetric coefficient of thermal expansion
β^* Volumetric coefficient of expansion with concentration
ν Kinematic viscosity
ρ Density of the fluid
σ Electric conductivity
μ Coefficient of viscosity
θ Dimensionless temperature
τ Dimensionless skin-friction.

Subscripts:

w Conditions on the wall
∞ Free stream conditions.

References:

[1] Gupta A S, Pop I and Soundalgekar V M. Free convection effects on the flow past an accelerated vertical plate in an incompressible dissipative fluid, Rev. Roum. Sci. Techn. Mec. Apl., 24(1979), 561-568.
[2] Sing A K and Kumar N. Free convection flow past an exponentially accelerated vertical plate, Astrophysics and Space Science, 98(1984), 245-258.
[3] Jha B K. MHD Free convection and mass transform flow through a porous medium}, Astrophysics and Space Science, 175(1991), 283-289.
[4] Jha B K, Prasad R and Rai S. Mass transfer effects on the flow past an exponentially accelerated vertical plate with constant heat flux, Astrophysics and Space Science,181(1991), 125-134.
[5] Kumar A G V and Verma S V K. Radiation effects on MHD flow past an impulsively started exponentially accelerated vertical plate with variable temperature in the presence of heat generation, Vol. 3, No. 4, 2011, pp. 2897-2909.
[6] Hossain M A and Shayo L K. The skin-friction in the unsteady free convection flow past an exponentially accelerated plate, Astrophysics and Space Science, 125(1986), 315-324.
[7] Kafousias N G, and Raptis A A. Mass transfer and free convection effects on the flow past an accelerated vertical plate with variable suction or injection, Rev. Roum. Sci. Techn. Mec. Apl., 26(1981), 11-22.
[8] Muthucumaraswamy R, Sathappan K E and Natarajan R. Mass transfer effects on exponentially accelerated isothermal vertical plate}, Int. J. of Appl. Math. and Mech., 4(6), 2008, 19-25.
[9] Reddy G V R, Murthy C V R and Reddy N B. Mixed convective MHD flow and mass transfer past an accelerated infinite vertical porous plate}, Mathematics applied in science and technology , 1(2009), 65-74.
[10] Rajput U S and Sahu P K. Transient free convection MHD flow between two long vertical parallel plates with constant temperature and variable mass diffusion, Int. Journal of Math. Analysis, 5(34), 2011, 1665-1671.
[11] Rajput U S and Sahu P K. Transient free convection MHD flow between two long vertical parallel plates with variable temperature and uniform mass diffusion in a porous medium, ARPN J. of Eng. and Applied Science, Vol. 6, No. 8, 2011, pp. 79-86.
[12] Rajput U S and Sahu P K. Combined effects of chemical reactions and heat generation or absorption on unsteady transient free convection MHD flow between two long vertical parallel plates through a porous medium with constant temperature and mass diffusion, Elixir Appl. Math., 39(2011), pp. 4855-4859.
[13] Rajput U S and Sahu P K. Radiation effects on steady hydromagnetic flow of a viscous fluid through a vertical channel in a porous medium with heat generation or absorption, Int. J. of Math. Archive, 2(10) (2011), pp. 1-7.

[14] Rajesh V. MHD effects on free convection and mass transform flow through a porous medium with variable temperature, Int. J. of Appl. Math. and Mech., 6(14)(2010), pp.1-16.
[15] Soundalgekar V M, Birajdar N S and Darwhekar V K, Mass transfer effects on the flow past vertical plate with variable temperature or constant heat flux, Astrophysics and Space Science, 100(1984), pp. 159-164.

Table 1: Skin-friction for different values of M

Pr	Sc	M	K	t	a	F	Gr	Gm	τ
0.71	0.6	1.0	0.5	0.2	0.5	1.0	10.0	5.0	1.30138
0.71	0.6	2.0	0.5	0.2	0.5	1.0	10.0	5.0	1.12692
0.71	0.6	3.0	0.5	0.2	0.5	1.0	10.0	5.0	0.98068
0.71	0.6	1.0	0.5	0.2	0.5	1.0	-10.0	-5.0	2.33783
0.71	0.6	2.0	0.5	0.2	0.5	1.0	-10.0	-5.0	2.14357
0.71	0.6	3.0	0.5	0.2	0.5	1.0	-10.0	-5.0	1.97857

Table 2: Skin-friction for different values of F

Pr	Sc	M	K	t	a	F	Gr	Gm	τ
0.71	0.6	1.0	0.5	0.2	0.5	1.0	10.0	5.0	1.30138
0.71	0.6	1.0	0.5	0.2	0.5	2.0	10.0	5.0	1.30417
0.71	0.6	1.0	0.5	0.2	0.5	3.0	10.0	5.0	1.30682
0.71	0.6	1.0	0.5	0.2	0.5	1.0	-10.0	-5.0	2.33783
0.71	0.6	1.0	0.5	0.2	0.5	2.0	-10.0	-5.0	2.33504
0.71	0.6	1.0	0.5	0.2	0.5	3.0	-10.0	-5.0	2.33239

Table 3: Skin-friction for different values of Pr and Sc.

Pr	Sc	M	K	t	a	F	Gr	Gm	τ
0.71	0.6	1.0	0.5	0.2	0.5	1.0	10.0	5.0	1.30138
3.0	0.6	1.0	0.5	0.2	0.5	1.0	10.0	5.0	1.40851
7.0	0.6	1.0	0.5	0.2	0.5	1.0	10.0	5.0	1.46586
0.71	0.6	1.0	0.5	0.2	0.5	1.0	-10.0	-5.0	2.33783
3.0	0.6	1.0	0.5	0.2	0.5	1.0	-10.0	-5.0	2.23070
7.0	0.6	1.0	0.5	0.2	0.5	1.0	-10.0	-5.0	2.17335
0.71	2.01	1.0	0.5	0.2	0.5	1.0	10.0	5.0	1.36075
0.71	2.01	1.0	0.5	0.2	0.5	1.0	-10.0	-5.0	2.2784

Table 4: Skin-friction for different values of a and K

Pr	Sc	M	K	t	a	F	Gr	Gm	τ
0.71	0.6	1.0	0.5	0.2	0.2	1.0	10.0	5.0	1.12404
0.71	0.6	1.0	0.5	0.2	0.5	1.0	10.0	5.0	1.30138
0.71	0.6	1.0	0.5	0.2	0.9	1.0	10.0	5.0	1.56010
0.71	0.6	1.0	0.5	0.2	0.2	1.0	-10.0	-5.0	2.16049
0.71	0.6	1.0	0.5	0.2	0.5	1.0	-10.0	-5.0	2.33783
0.71	0.6	1.0	0.5	0.2	0.9	1.0	-10.0	-5.0	2.59654
0.71	0.6	1.0	0.3	0.2	0.5	1.0	10.0	5.0	1.63789
0.71	0.6	1.0	1.0	0.2	0.5	1.0	10.0	5.0	1.03274
0.71	0.6	1.0	0.3	0.2	0.5	1.0	-10.0	-5.0	2.64314
0.71	0.6	1.0	1.0	0.2	0.5	1.0	-10.0	-5.0	2.09011

Table 5: Skin-friction for different values of Gr and Gm.

Pr	Sc	M	K	t	a	F	Gr	Gm	τ
0.71	0.6	1.0	0.5	0.2	0.5	1.0	5.0	5.0	1.47305
0.71	0.6	1.0	0.5	0.2	0.5	1.0	10.0	5.0	1.30138
0.71	0.6	1.0	0.5	0.2	0.5	1.0	15.0	5.0	1.12972
0.71	0.6	1.0	0.5	0.2	0.5	1.0	-5.0	-5.0	2.16616
0.71	0.6	1.0	0.5	0.2	0.5	1.0	-10.0	-5.0	2.33783
0.71	0.6	1.0	0.5	0.2	0.5	1.0	-15.0	-5.0	2.50949
0.71	0.6	1.0	0.5	0.2	0.5	1.0	10.0	10.0	1.12649
0.71	0.6	1.0	0.5	0.2	0.5	1.0	10.0	15.0	0.95160
0.71	0.6	1.0	0.5	0.2	0.5	1.0	-10.0	-10.0	2.51272
0.71	0.6	1.0	0.5	0.2	0.5	1.0	-10.0	-15.0	2.68761

Table 6: Nusselt Number

t	Pr	Nu
0.2	0.71	0.425206
0.2	3.0	0.874039
0.2	7.0	1.335120
0.4	0.71	0.601332
0.6	0.71	0.736478

Table 7: Shrewood Number

F	Sc	t	Sh
1.0	0.6	0.2	0.416434
2.0	0.6	0.2	0.441028
3.0	0.6	0.2	0.464739
1.0	0.6	0.4	0.623707
1.0	0.6	0.6	0.804951
1.0	0.78	0.2	0.474808
1.0	2.01	0.2	0.762200